Journal of the Taiwan Institute of Chemical Engineers 45 (2014) 579–588

Contents lists available at SciVerse ScienceDirect

Journal of the Taiwan Institute of Chemical Engineers

journal homepage: www.elsevier.com/locate/jtice

Adsorptive removal of CO_2 on highly microporous activated carbons prepared from *Eucalyptus camaldulensis* wood: Effect of chemical activation

Aghdas Heidari [a], Habibollah Younesi [a,*], Alimorad Rashidi [b], AliAsghar Ghoreyshi [c]

[a] Department of Environmental Science, Faculty of Natural Resources & Marine Science, Tarbiat Modares University, Imam Reza Street, P.O. Box 46414-356, Noor, Iran
[b] Nanotechnology Research Center, Research Institute of Petroleum Industry (RIPI), West Blvd. Azadi Sport Complex, P.O. Box 14665-1998, Tehran, Iran
[c] Department of Chemical Engineering, Babol University of Technology, Babol, Iran

ARTICLE INFO

Article history:
Received 20 February 2013
Received in revised form 8 May 2013
Accepted 3 June 2013
Available online 4 July 2013

Keywords:
Eucalyptus wood
Activated carbon
Pyrolysis
Chemical activation
CO_2 adsorption

ABSTRACT

A series of activated carbons (ACs) were prepared from *Eucalyptus camaldulensis* wood by chemical activation with H_3PO_4, $ZnCl_2$ at different impregnation ratios as well as by pyrolysis, followed by activation with KOH. The porosity characteristics of these ACs were determined by N_2 adsorption isotherms. Through varying the H_3PO_4/biomass ratio from 1.5 to 2.5, the prepared ACs displayed BET surface areas in the range of 1875–2117 m^2/g with micropores content of 69–97%. For the $ZnCl_2$ activated series, BET surface areas varying from 1274.8 to 2107.9 m^2/g with micropores content of 93–100% were obtained from impregnation ratios of 0.75–2.0. The AC obtained by KOH had the largest BET surface area of 2594 m^2/g and the high micropore content of 98%. In addition, the FTIR and SEM analyses conducted for characterizing the ACs and the CO_2 adsorption onto all series of the eucalyptus wood based ACs at pressures ranging from 0 to 16 bar using a volumetric method were investigated. Also the effect of temperature (15–75 °C) on the amount of CO_2 adsorbed by the ACs that was prepared with H_3PO_4, KOH and $ZnCl_2$ was studied. The CO_2 adsorption capacity on the AC prepared with KOH was up to 4.10 mmol/g at 1 bar and 303 K, having an increase of about 63% in comparison with the commercial AC.

1. Introduction

Activated carbon is an extremely versatile carbonaceous material that is widely used as adsorbent, catalyst and catalyst support in industries [1,2]. Moreover, its large surface area and micropore volume, favorable pore size distribution, surface chemistry including the oxygen functional groups, the degree of polarity and the active surface area lend AC appropriate as adsorbent for a variety of environmental applications, i.e. purification and storage of gases, removal of organic materials and metals from aqueous solution [3,4]. The adsorption efficiency of AC relies strongly on its special surface and structural characteristics. For example, AC utilized for the adsorption of gases and vapors should consist of pores with effective radii, significantly smaller than 16–20 Å [5,6].

Activated carbon is mainly produced by thermal and chemical activation. Thermal or physical activation involves the primary carbonization of a carbonaceous precursor (below 700 °C) followed by the activation of the obtained char with oxidizing gases such as air, CO_2 or steam at high temperature in the range of 700–1100 °C. Chemical activation consists of the impregnation of raw material with chemical agents such as H_3PO_4, $ZnCl_2$ or KOH followed by carbonization at temperatures between 400 and 800 °C under a nitrogen atmosphere [4,7,8]. It is well-known that AC can be prepared by pyrolysis from a wide range of different carbon-containing source materials [7]. An enormous range of lignocellulosic materials including rice husk [9], corn cobs [9,10] fruit stone [11,12], date stone [13], almond shell [14], coconut shell [15], sugar cane bagasse [16], palm shell [3], pistachio-nut shell [17,18] and cotton stalk [7] have been used as activated carbon precursors. *Eucalyptus camaldulensis* wood is a kind of lignocellulosic material which has a reasonably high content of carbon, utilized also as raw material for AC [19,20]. In this study, the potential of *E. camaldulensis* wood as precursor for the preparation of AC by chemical activation was investigated. Over the past years, a few reports have been published on preparation of AC from different parts of the *Eucalyptus* species; Patnukao [19] prepared AC with *E. camaldulensis* Dehn bark using phosphoric acid activation. Tancredi *et al.* [21] used *Eucalyptus grandis* sawdust for production of AC with CO_2, CO_2–O_2 and steam activation. Elyounssi *et al.* [22]

* Corresponding author. Tel.: +98 0122 625 3101 3; fax: +98 0122 625 3499.
E-mail addresses: hunesi@modares.ac.ir, hunesi@yahoo.com (H. Younesi).

1876-1070/$ – see front matter © 2013 Taiwan Institute of Chemical Engineers. Published by Elsevier B.V. All rights reserved.
http://dx.doi.org/10.1016/j.jtice.2013.06.007

improved the charcoal yield by two-step pyrolysis of eucalyptus wood. In addition, Ngernyen *et al.* [20] reported the production of AC from eucalyptus wood by CO_2 activation.

Techniques are employed for producing effective AC from agriculture waste, which include physical treatment; heat treatment, ammonia gas treatment (amination and ammoxidation) and chemical treatment; impregnation (prior to carbonization) of chemicals. The main objective of present was to prepare AC from *Eucalyptus camendalisis* wood with highly microporous and large specific surface area that considered highly potential adsorbent for CO_2 adsorption. Therefore, we reported the synthesis of AC with high specific surface area and high micropore volume from agricultural waste materials. We carried out the experiments based on the impregnation procedure since the lower temperatures and shorter time needed for activating carbon. Moreover, the adsorptive capacity of the AC can be efficiently increased by chemical impregnation which together with the surface area, pore size distribution and surface chemistry of AC. Previously, it has been reported by Romanos *et al.* [23] that AC with high specific surface area, porosities, nanometer pore volumes achieved by the chemical impregnation methods of KOH and H_3PO_4. In addition, it has been found by Khalili *et al.* [6] that the effect of impregnation of AC from paper mill sludge with $ZnCl_2$ promoted microporosity of AC by controlling the amount of zinc. Besides that, a few works studied the synthesis of AC from Eucalyptus wood with phosphoric acid. However, to our knowledge, there is a lack of information in the literature about the preparation of AC from Eucalyptus wood by the chemical impregnation of $ZnCl_2$ and KOH as activating agent and also their application for CO_2 adsorbent.

Carbon dioxide, a major green house gas emitted by the combustion processes of fossil fuels (coal, oil and natural gas) in industrial plants [24], has received much attention recently due to its adverse impacts on climate change and global warming [25,26]. Presently, a wide range of techniques including absorption, adsorption, and membranes have been suggested to sequestrate CO_2 from fuel gases [25,26]. Therefore, adsorption is regarded as a promising and economic technique due to its low energy requirement, cost effectiveness and ease of use at wide variety of temperatures and pressures [26]. A lot of absorbents have been studied for CO_2 adsorption including zeolites, carbon nanotube, activated carbons, silicas, hydrotalcites, metal oxides, MOFs, *etc.* [27–30]. Among the many well-known adsorbents, AC is widely employed for CO_2 adsorption due to its large surface area, porous structure, lesser sensitivity to moisture, availability, low cost and easy regeneration with low energy requirement [25,31,32]. Activated carbon is an outstanding adsorbent and commonly used for adsorption of CO_2 [26,31,33,34]. However, most ACs displayed low CO_2 adsorption capacity, making it inappropriate for this application [26,31,32,35]. A technique that has been investigated to improve the CO_2 uptake capacity is to make porous carbon with a tailored pore structure, appropriate for CO_2 adsorption.

The main objective of the present work is to prepare porous activated carbon from eucalyptus wood with a narrow pore size distribution and a large surface area for CO_2 adsorption by chemical activation of H_3PO_4, $ZnCl_2$ and extra activation with KOH. The influence of different impregnation ratios of $ZnCl_2$ and H_3PO_4 on the pore structure and the CO_2 adsorption capacity of the prepared AC was investigated. In addition, for creating a AC adsorbent with a large number of nanometer pores and a large surface area and for increasing the CO_2 adsorption capacity, an AC sample with a large surface area activated with KOH in a multi-step activation process, along with its pore characteristics was studied. Furthermore, the effect of temperature on the CO_2 capture capacity onto AC from eucalyptus wood was examined.

2. Materials and methods

2.1. Materials

Eucalyptus wood was used as raw material for the preparation of AC. The eucalyptus wood (*E. camaldulensis*) was obtained from a waste dump of a wood factory in the north of Iran. The collected eucalyptus wood was crushed to pulp, then dried in an air oven at 70 °C and finally smashed and sieved to particle size of 0.4–0.8 mm.

2.2. Preparation of activated carbon

Activated carbon was prepared by mixing a known weight of the eucalyptus wood (0.4–0.8 mm) with two different concentrations of H_3PO_4, with impregnation ratios of H_3PO_4: eucalyptus wood of 1.5, 2, and 2.5 g/g. After mixing both together, the acid impregnated material was dried overnight at 90 °C, then a weighed sample was carbonized in a quartz tube furnace at temperature of 450 °C, holding time of 1 h and heating rate of 4 °C/min. After carbonization, the sample was cooled down to room temperature in a flow of nitrogen and then removed from the reactor. In order to remove impurities in the synthesized, AC, it was dispersed in a solution of HCl and distilled water at 60 °C for 2 h. After that, the sample was washed sequentially with hot and cold distilled water until the wash water reached to pH of 6–7 and it was divided into 3 parts. Finally these samples were air dried at 70 °C, weighed and kept in bottles for subsequent use, designated as $H_{1.5}$, H_2, and $H_{2.5}$.

The preparation of AC with KOH was according to the method reported for corn cob [23]. In fact, the AC was prepared in a multi-step activation process with H_3PO_4 and KOH. In the first step, the activation process was done with H_3PO_4 as described above. In the second activation step, the resulting char was mixed for 1 h with KOH solution, using KOH:C weight ratio of 3.5. After that, the slurry was dried at 70 °C for 24 h. The dried sample was then pyrolyzed in a ceramic tube furnace at temperature of 900 °C, holding time of 1 h and heating rate of 5 °C/min. The obtained AC was washed with hot and cold distilled water until pH of 6–7 was attained. Finally, it was dried at 70 °C and labeled HK.

The preparation of AC from eucalyptus wood, using $ZnCl_2$ as activating agent followed the procedure reported by [6] for a paper mill sludge. In a similar manner, a known mass of $ZnCl_2$ was first mixed with the eucalyptus wood in a way to provide $ZnCl_2$ to biomass impregnation ratios of 0.75, 1.5, and 2.5 g/g in 3 samples. The obtained slurry was kept at 85 °C for 7 h to ensure a complete reaction between them. For removing residual water, the treated samples were then dried overnight at 110 °C. After that, samples were pyrolyzed in a quartz tube furnace at temperature of 500 °C, holding time of 2 h and heating rate of 15 °C/min. The resulting char samples were washed according to the method mentioned above for H_3PO_4 activated samples. They were then labeled as $Z_{0.75}$, $Z_{1.5}$, and $Z_{2.5}$. Table 1 summarizes pyrolysis parameters for activated carbon prepared from Eucalyptus wood.

Table 1
Some preparation parameters of activated carbon.

Samples	Activating agent	Impregnation ratio, agent-to raw, by weight	Carbonization temperature (°C)	Carbonization time (h)	Heating rate (°C/min)
$H_{1.5}$	H_3PO_4	1.5	450	1	4
H_2	H_3PO_4	2	450	1	4
$H_{2.5}$	H_3PO_4	2.5	450	1	4
HK	KOH	3.5	900	1	5
$Z_{0.75}$	$ZnCl_2$	0.75	500	2	15
$Z_{1.5}$	$ZnCl_2$	1.5	500	2	15
$Z_{2.5}$	$ZnCl_2$	2.5	500	2	15

2.3. Characterization of the AC samples

The textural characterization of the prepared AC included the surface area, the extent of micro- and mesoporosity, while the pore size distribution was conducted using N_2 adsorption/desorption at 77 K using Micromeritics ASAP 2010. The specific surface areas were calculated from the N_2 adsorption isotherm with Brunauer, Emmet and Teller (BET) equation at the relative pressure in the range of 0.001–0.3 bar. The total pore volume was determined from the amount of N_2 adsorbed at P/P 0 0.99. The volume of micropores was estimated using the MP method, calculated by subtracting the micropore volume from the total pore volume. The mesopore volume distribution was calculated according to BJH method. It should be mentioned that prior to all adsorption measurements, the AC samples were degassed at 250 °C under vacuum for 2 h.

The surface functional groups of the AC samples were detected by Fourier Transform Infrared (FTIR) spectroscope (FTIR – AVATAR 370, Thermo Nicolet) using a potassium bromide (KBr) pellet prepared by mixing 0.033% of dried AC sample in KBr (Fluka Co.). The spectra were recorded between 4000 and 400 cm^{-1}. The surface morphology of the AC was examined using a scanning electron microscopy (SEM). The AC sample was covered with gold by a gold sputtering device to provide a better visibility of the surface morphology. Thermogravimetric analysis (TGA) of the eucalyptus wood was conducted by using a thermogravimetric analyzer (Rheometric Scientific STA 1500) under N_2 atmosphere, from room temperature to 800 °C at the heating rate of 10 °C/min.

2.4. CO_2 adsorption measurement

The CO_2 adsorption experiments on the AC were performed by using a volumetric adsorption set up. Fig. 1 shows the schematic diagram of the volumetric apparatus. It included two stainless steel sample cells (an adsorption cell and a gas cell), a set of valves and a couple of high precision pressure transducers (maximum pressure 60 bar). The gas and adsorption cell volumes were 144 ml and 30 ml, respectively. In order to keep the temperature constant during the gas adsorption experiment, the gas cell and the adsorption cell were placed in a thermostatic water bath along with a water circulating system (77960 Seelbach, Julabo Co, Germany). Furthermore, before starting each CO_2 adsorption experiment, the set up was leak tested using helium gas (He) at 35 bars pressure.

Prior to each adsorption experiment, the adsorption cell was cleaned and 1 g of the adsorbent, degassed at 150 °C for about 24 h, was put in it. The system was evacuated for 2 h with a vacuum pump. The adsorption experiments were carried out at pressures ranging from 0 to 16 bar at four different temperatures (15, 30, 45, and 75 °C). For determination of the dead volume of the whole set up, helium gas was used as non-adsorbing gas and expanded to the gas cell and then the adsorption cell. The total amount of CO_2 introduced into the system and remaining after reaching adsorption equilibrium was determined by measuring the volume of the gas cell, the CO_2 pressure before and after adsorption, and the temperature of the system. The CO_2 adsorption capacity of the AC adsorbent was calculated by using the ideal gas law and with help of the MATLAB software.

2.5. Adsorption isotherms

The Langmuir and Freundlich models are the most frequently employed models to explain experimental equilibrium data of adsorption isotherms. The Langmuir model is initially designed for the adsorption of gas molecules onto solids, assuming that the adsorption phenomenon happens in a monolayer and all adsorption sites are similar and energetically equivalent. Therefore, the Langmuir equation is depicted by the following Eq. (1) [36].

$$q = q_m \frac{b\,p}{1 + bP} \tag{1}$$

where P is the equilibrium pressure and q_m and b are constant Langmuir isotherms, indicating the maximum adsorption capacity and the energy of adsorption, respectively.

The Freundlich adsorption equation is an empirical model that is commonly described by the following nonlinear Eq. (2) [13].

$$q = k\,p^n \tag{2}$$

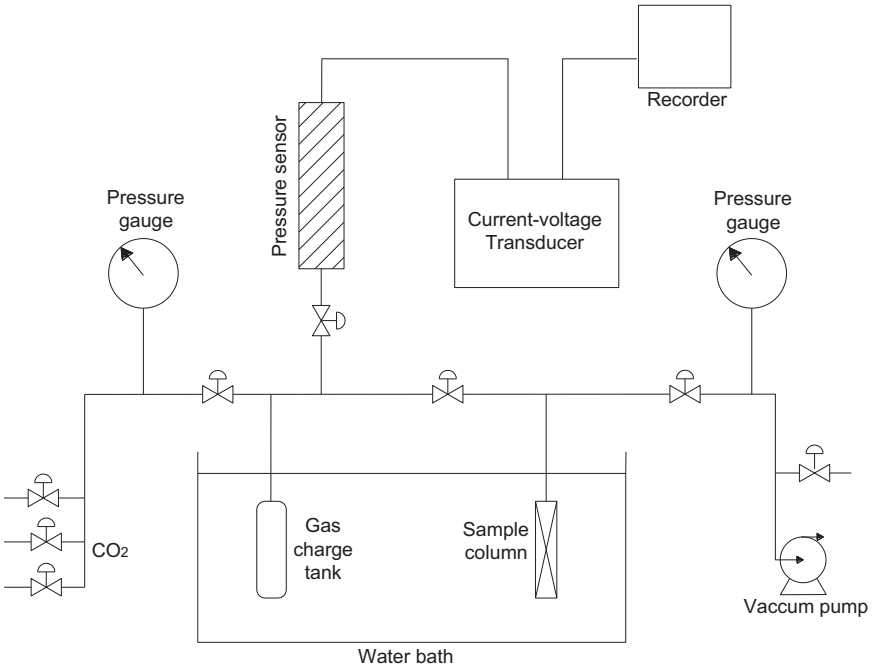

Fig. 1. Schematic diagram of the CO_2 adsorption apparatus.

Table 2
Ultimate and proximate analysis of Eucalyptus wood.

Proximate analysis	Wt%	Ultimate analysis, dry basis	Wt%
Moisture	5	Sulfur	<0.1
Volatile matter	80.48	Carbon	48.2
Ash	4.8	Hydrogen	6.2
Fixed carbon	14.65	Nitrogen	<0.5
		Oxygen	44.1

where k and n are Freundlich isotherm parameters, representing the adsorption capacity and the adsorption intensity, respectively.

3. Results and discussion

3.1. Properties of raw materials

The characteristics of *E. camaldulensis* wood were analyzed with ASTM techniques. The values of the ultimate (carbon, hydrogen, nitrogen and sulfur) and proximate (moisture, volatile matter, fixed carbon and ash content) analysis of the eucalyptus wood sample based on the average of three samples were analyzed in each replica. In the proximate analysis, the contents of moisture (5%), volatile matter (80.48%), ashes (4.8%) and fixed carbon (14.65%) were determined. In the ultimate analysis, dry wood had and elemental composition of about 48.2% carbon (C), 6.2% hydrogen (H), 0.5% nitrogen (N), 0.1% sulfur (S) and 44.1% oxygen (O) (calculated by difference). Table 2 shows the ultimate and proximate analysis of the used Eucalyptus wood.

The thermal behavior of eucalyptus wood biomass was examined by TGA (figure not shown). The pyrolysis of eucalyptus wood, like that of any other biomass comprised mainly of hemicelluloses, cellulose, and lignin, is associated with the pyrolysis of these polymers [37]. The TGA curve indicates three mass loss steps; the evaporation of adsorbed moisture up to 110 °C, the decomposition of hemicelluloses in the biomass at 250–340 °C, and the cellulose decomposition at about 380–520 °C [20].

3.2. Pore structure development

The characterization of the pore structure of the adsorbents is commonly determined by the adsorption of inert gases [18]. Adsorption–desorption isotherms of N_2 at 77 K and BJH pore size distribution of the AC prepared from eucalyptus wood by $ZnCl_2$ and H_3PO_4 and KOH are shown in Fig. 2. The textural properties of the AC prepared with H_3PO_4, KOH, and $ZnCl_2$, including S_{BET}, V_{mic}, V_{mes}, V_{total}, R_p and yield are listed in Table 3. The type of the activating agent and the impregnation ratio seems to have a significant influence on the shape of the N_2 adsorption–desorption isotherms (Fig. 2). According to IUPAC classification, the isotherms of eucalyptus wood impregnated with H_3PO_4 and $ZnCl_2$ at the lowest ratio (1.5) and KOH are typical Type I adsorption isotherms, which

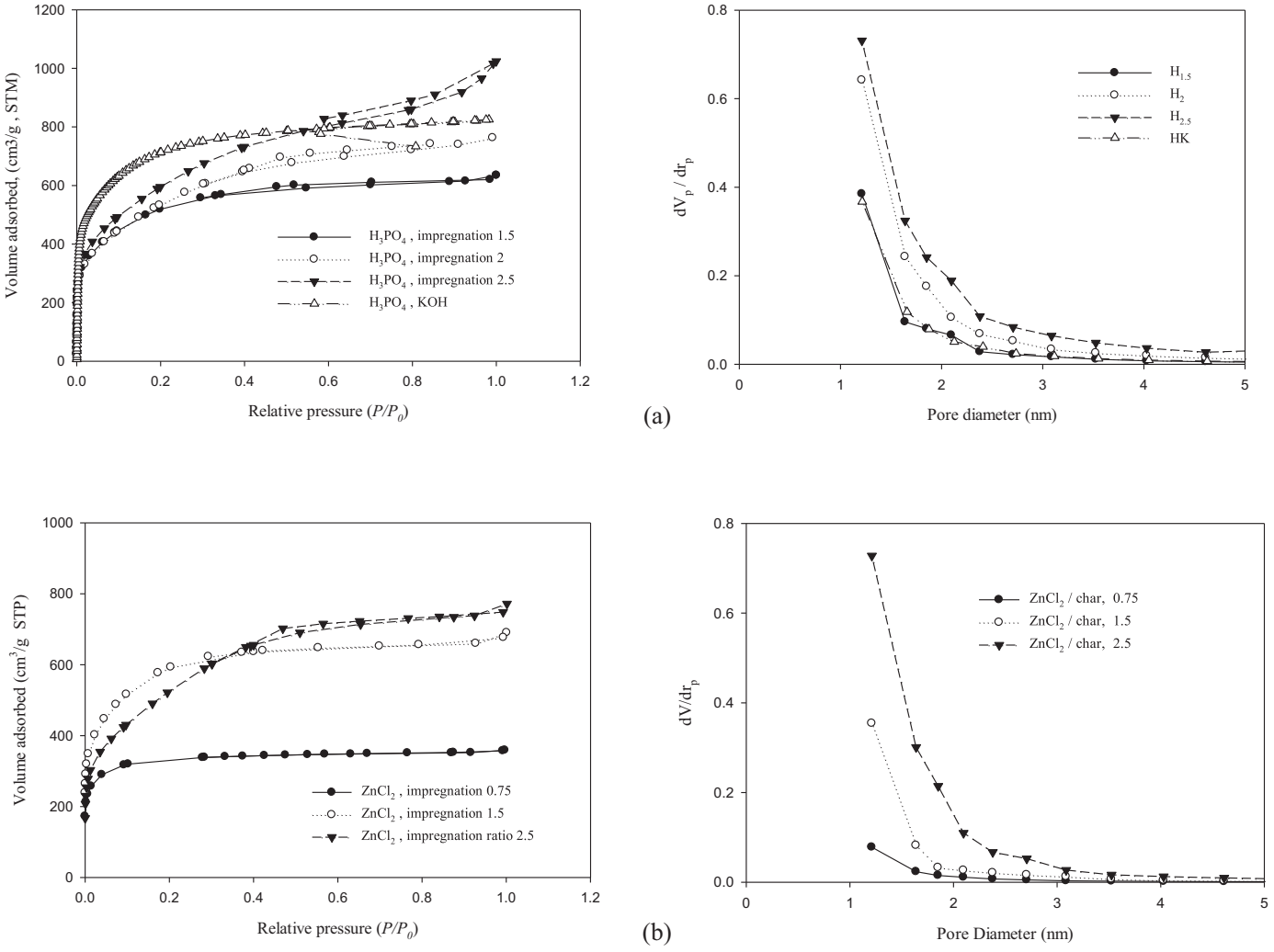

Fig. 2. Adsorption–desorption isotherms of N_2 at 77 K and BJH pore size distribution of activated carbon prepared with (a) H_3PO_4 and KOH and (b) $ZnCl_2$.

Table 3
Textural parameters of the prepared activated carbon.

Sample	Activating agent	Impregnation ratio	Yield (%)	Textural parameters					
				S_{BET} (m^2/g)	V_{mic} (cm^3/g)	V_{mes} (cm^3/g)	V_{total} (cm^3/g)	R (nm)	V_{mic} (%)
$H_{1.5}$	H_3PO_4	1.5	50	1875	0.949	0.027	0.976	2.083	97
H_2	H_3PO_4	2	50	1889	1.063	0.114	1.178	2.495	90
$H_{2.5}$	H_3PO_4	2.5	48.8	2117	1.088	0.469	1.557	2.943	69
HK	H_3PO_4, KOH	2, 3.5	23.8	2595	1.236	0.039	1.275	1.966	98.7
$Z_{0.75}$	$ZnCl_2$	0.75	34	1275	0.568	0.000	0.553	1.73	100
$Z_{1.5}$	$ZnCl_2$	1.5	29	2108	1.046	0.013	1.059	2.01	98
$Z_{2.5}$	$ZnCl_2$	2.5	29	1794	1.109	0.075	1.184	2.64	93

dramatically increase at low relative pressure and reach a horizontal plateau. This indicates that the AC samples should exhibit narrow pore size distribution on micropore range. As the impregnation ratio of $ZnCl_2$ and H_3PO_4 was raised, the slope of the curve gradually increased and the isotherms exhibited hysteresis loops. Thus, the isotherms appear to become a combination of Type I and IV according to IUPAC classification and, for the isotherms of prepared AC with the highest impregnation ratio, it moves toward a Type IV isotherm. This can be attributed to formation of a greater fraction of mesoporosity, which is proved by the mesopore volume in Table 3.

The majority of the ACs prepared in this research was basically microporous, because more than 90% of the total pore volume was included within this range. This statement is confirmed by analyzing the pore size distribution with the BJH theory. Fig. 2 shows also the BJH pore size distribution for the AC derived from eucalyptus wood with $ZnCl_2$, H_3PO_4 and KOH at different impregnation ratios. It can be seen that the pore size distribution of the AC samples are similar and more narrowly distributed and mainly composed of micropores. It is good to mention that adsorbent pores are classified as micropore (diameter < 2 nm), mesopore ($2 <$ diameter < 50 nm) and macropore (diameter > 50 nm) [18,38].

According to Table 3, when H_3PO_4 was used as the activating agent, an increase in the impregnation ratio increased the BET surface area and mesoporosity. This is due to the fact that the activating agent decreases the formation of tars and any other liquids that cause blocking of the pores and prevent the growth of porous structures in the AC [39]. In the case of sample HK, the AC that used H_3PO_4 and KOH as activating agent had a larger BET surface area up to 2594 m^2/g compared to all of the prepared samples. The obtained maximum BET surface area is attributed to the decline of O_2, H_2, and N_2 contents of the biomass during successive activation steps, creating a nanoporous carbon adsorbent with high porosity and surface area for gas application [23]. Furthermore, the BET surface area and mesoporosity of the AC samples prepared with $ZnCl_2$, decreased with a rising impregnation ratio due to transformation of the micropores to mesoporous ones [6]. For comparison, as-prepared AC from *E. camaldulensis* had relatively high surface area of from 1870 to 2100 m^2/g while Patnukao and Pavasant [19], with the same activating agent as in this work, obtained AC from *Eucalyptus* bark for its adsorption capacity for Cu(II) and Pb(II) with a maximum surface area of 1239 m^2/g. Nevertheless, the BET surface area and total pore volume values obtained in the present study were relatively high compared with those published previously in the literature (Table 3).

It is mentioned in the literature that the type of precursor and the activation conditions have influence on the microporosity of the AC [40]. The porosity is created by chemical compounds remaining intercalated in the internal structure of lignocellulosic materials, hindering their shrinkage [40–42]. In the case of activation with H_3PO_4, the phosphoric acid and its derivates (polyphosphoric acid) interact with the organic matter present in the biomass to form phosphate linkage such as phosphate and polyphosphate esters, which can serve to connect and crosslink biopolymers. The pores are generated by the formation of these linkages which expand the biomass structure [4]. The polyphosphate compounds have bigger size than $ZnCl_2$, which fills a wide range of pore sizes and leads to creation of large sized mesopores, but then $ZnCl_2$ and its hydrates mostly cause the small and uniform size of the microporous ones [40].

The obtained results in this study are in agreement with the findings of other similar research efforts. Timur et al. [40] prepared AC from oak cup pulp by chemical activation with H_3PO_4 and $ZnCl_2$. Their results showed that zinc chloride caused the AC to have higher micropore volume compared to activation by phosphoric acid. In addition, researchers used H_3PO_4, $ZnCl_2$, and KOH for preparing AC from peach stone and observed that although the three activating agents produce a high incidence of microporosity, there is a degree of macroporosity among them, as well [43]. With H_3PO_4 large mesopores and even macropores were produced, while with $ZnCl_2$ both wide micropores and low mesopores were created. The results from a study also demonstrated that the maximum limit of micropores attained by the KOH activated cotton stalk was comparable with the smallest value for the H_3PO_4 treated sample [7].

3.3. SEM analysis of activated carbon

The SEM images of the AC samples derived from eucalyptus wood with $ZnCl_2$, and H_3PO_4 are shown in Fig. 3. As shown in these figures, pores of different size and different morphology within the structure of the AC samples, with mesopores and micropores hiding inside the ACs. It should be noted that the external surface of the AC samples prepared by H_3PO_4 have larger pore size compared to the other AC samples. The reason could be the evaporation of H_3PO_4 during carbonization leaving empty space previously occupied by H_3PO_4.

3.4. Surface functional groups

The chemical nature of the functional groups on the AC surface was identified with FTIR (Fig. 4a and b). The spectra of all the AC samples derived from eucalyptus wood with H_3PO_4, $ZnCl_2$, and KOH have many similar features. The bands located in the regions 3427, 3435, 3438, and 3440 cm^{-1} for all can be attributed to functional groups of–OH of phenol, alcohol, and carboxylic acid [7,12,23,31,44,45]. The relatively intense bands at about 1200, observed in all the samples activated with H_3PO_4 and $ZnCl_2$, are attributed to C–O–C stretching in ethers [7,44]. In the FTIR spectra the peaks observed at 1577 and 1586 cm^{-1} for the H_3PO_4 and $ZnCl_2$ activated AC samples and at 1542 for the KOH activated sample can be attributed to C=O stretching in ketones [44,46]. The C=O stretching in lactones can be found at 1700, 1703, and 1707 cm^{-1} in the spectra of the AC samples prepared with H_3PO_4 and $ZnCl_2$ [46].

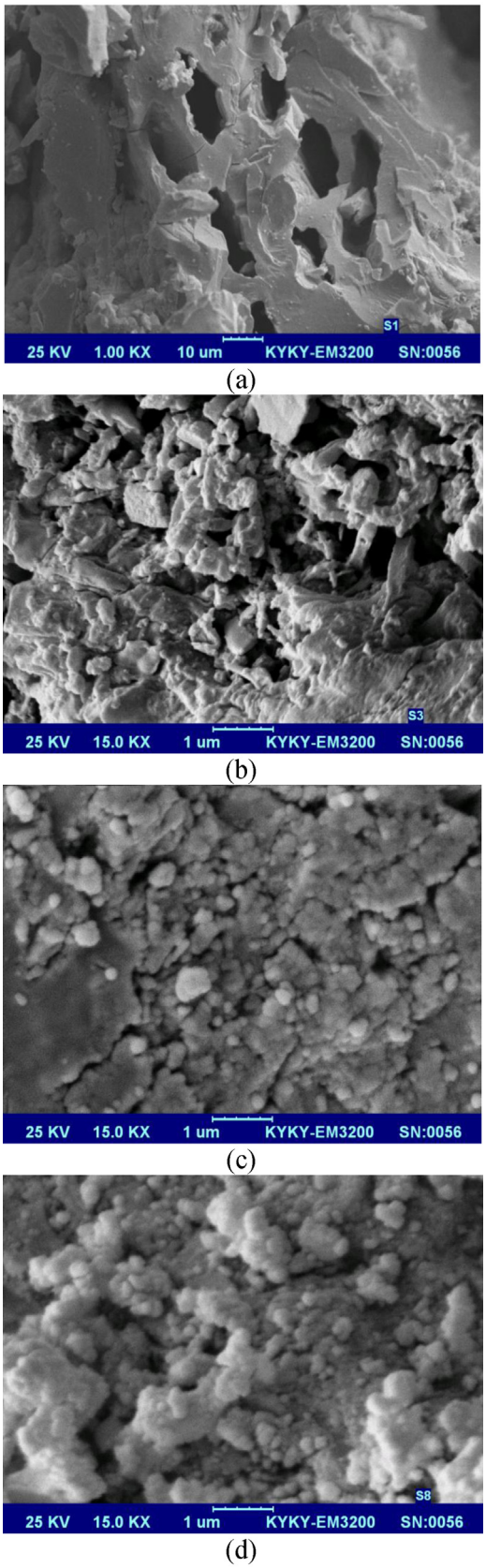

Fig. 3. SEM images of the activated carbon samples derived from eucalyptus wood with (a) $H_{1.5}$, (b) H_2, (c) $Z_{1.5}$, and (d) $Z_{2.5}$.

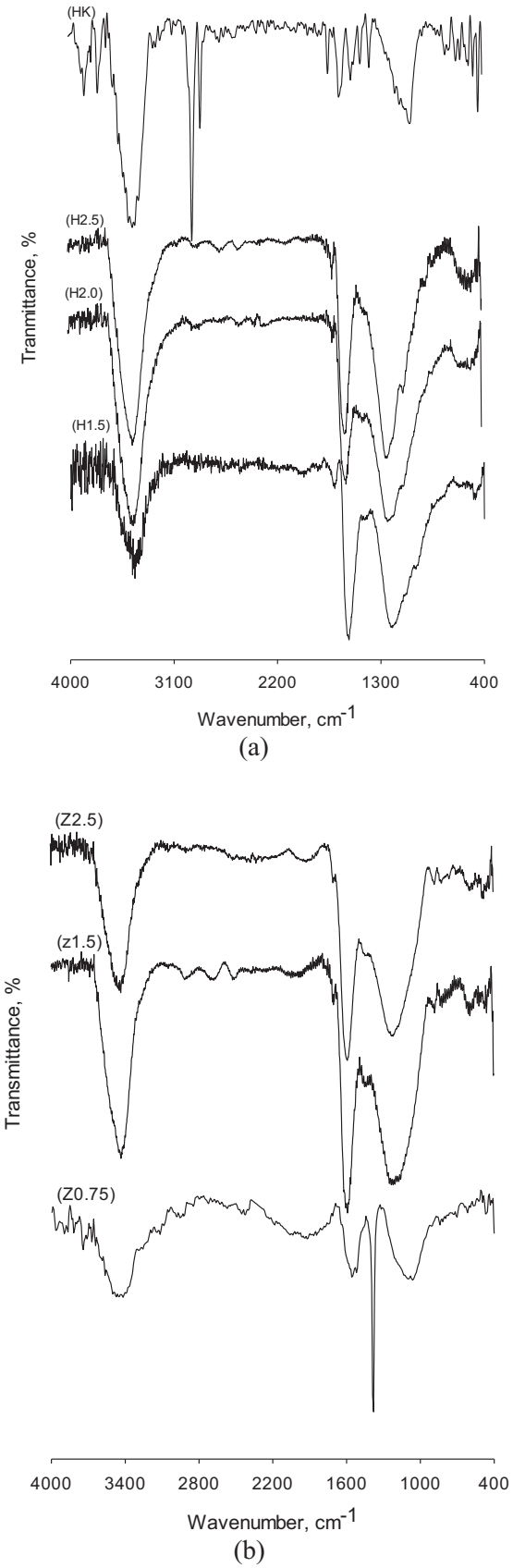

Fig. 4. FTIR spectra for the AC samples derived from Eucalyptus wood with (a) H_3PO_4, KOH, and (b) $ZnCl_2$.

The FTIR spectra of KOH-carbon exhibit some differences compared to other ACs. For example, the spectrum of the KOH-carbon shows a peak at 2854 and 2932 cm^{-1} that corresponds to the C–H bond stretching of carboxylic acids [46]. However, the other peak at 1643 cm^{-1} is due to quinines [46]. The new band located at 1026 cm^{-1} is ascribed to C–O–C stretching that may be present in ethers [44].

3.5. CO_2 adsorption onto the prepared AC

CO_2 is the green house gas that has attracted much attention of late [26]. Based on the literature, AC adsorbents have high adsorption capacity for CO_2 [15,26,31,47–49]. The CO_2 adsorption capacity of the ACs prepared with different impregnation ratios of the activating agents (H_3PO_4, $ZnCl_2$, and KOH) from eucalyptus wood were examined. The CO_2 adsorption isotherms of the AC samples are presented in Fig. 5a–e. The constants of the Langmuir and Freundlich models for the CO_2 adsorption are represented in Table 4. It can be seen that the amount of CO_2 adsorbed onto the AC samples prepared with $ZnCl_2$ ($Z_{1.5}$, Z_2 and $Z_{2.5}$) increases as the impregnation ratio of the activating agent to biomass decreases or, in other words, the CO_2 adsorbed onto the AC increases when the BET surface area and the mesoporosity of the AC samples increases. The $Z_{0.75}$ sample has the highest CO_2 adsorption capacity due to having the maximum percentage of micropores up to 100% (Table 4). Our results are in agreement with the research reported in the literature [3]. They prepared some granular AC from oil palm shell by $ZnCl_2$ for methane adsorption. Their results showed that increasing the $ZnCl_2$ impregnation ratio causes a decrease in methane adsorption due to the widening of the micropores and the formation of mesopores (Fig. 5a).

The CO_2 adsorption isotherms for AC samples prepared with H_3PO_4 are shown in Fig. 5b, where it can be seen how the CO_2 adsorption capacity of the AC samples increases when the impregnation ratio of H_3PO_4 to biomass is increased from 1.5 to 2 g/g ($H_{1.5}$ and H_2 samples) and then sharply decreases at the upper ratio 2.5 g/g ($H_{2.5}$ sample). Although the $H_{2.5}$ sample exhibits a maximum BET surface area, it has a substantially low CO_2 adsorption capacity, which can be attributed to the creation of more mesopore fractions and low microporosity (Table 4).

The AC sample activated with KOH (HK) showed the maximum CO_2 adsorption capacity. The improvement in CO_2 adsorption capacity of the HK sample contributed to the abundant formation of nanometer pores and the largest BET surface area. The reason can be described in this manner: the specific surface area and the micropore volume are strongly influenced by gas adsorption [50,51]. Normally, the gas molecules in the gas–solid interaction are adsorbed by strong van der Wals forces. Gas adsorption potential is at the maximum in the sub-nanometer when the gas molecules start to overlap with the reducing pore size, resulting in a much higher binding energy emanating from the formation of deep potential wells. Thus, it is crucial to increase the number of sub-nanometer pores, and decrease the number of supra-nanometer ones which automatically also leads to an increase in the specific surface area [23,52].

In the present study, it was observed that the HK sample (the AC by chemical activation using H_3PO_4 followed by chemical activation with KOH) exhibited relatively high adsorption capacity of up to 4.10 mmol/g at 1 bar and 303 K, compared with those obtained AC using other adsorbents. This led to an increase of about 63% in comparison with the commercial AC (Table 4). Furthermore, it should be mentioned that in this study the comparable CO_2 adsorption capacity of the AC prepared with H_3PO_4, $ZnCl_2$, KOH and the commercial AC are in the following order: HK > H_2 > $Z_{0.75}$ > commercial AC.

Langmuir and Freundlich models were employed to describe the adsorption data of CO_2 onto the AC derived from eucalyptus wood at different impregnation ratios and temperatures, as shown in Fig. 5c and d. All the CO_2 adsorption isotherms attributed to Type I of IUPAC classification are typical of microporous materials. It can be seen that good agreement noticed between the experimental data and the fitting of both models indicates that these models can accurately explain the correlation of the adsorption equilibrium with the adsorbent. In the most of cases, the obtained regression coefficient R^2, higher than 0.98, indicates good agreement between the experimental CO_2 adsorption data and the theoretical predictions. The effect of temperature on the amount of CO_2 adsorbed onto the ACs prepared with H_3PO_4, KOH and $ZnCl_2$ from eucalyptus wood was investigated. According to Table 4 and Fig. 5c–e, the CO_2 maximum adsorption capacity, q_m, decreases from 30.2 to 7.7 mmol/g, from 37.9 to 15.8 mmol/g and from 65.3 to 22.7 mmol/g for H_3PO_4, $ZnCl_2$ and KOH, respectively, with the increase of temperature. On the other hand, the amounts of CO_2 adsorbed onto the prepared AC samples declined significantly with the rising temperature and the lower temperature had the larger CO_2 adsorption capacity which indicated that the CO_2 adsorption onto the AC was mostly physical adsorption.

3.6. Comparison of CO_2 adsorption capacities with other type of activated carbon

Several studies reported in the literature indicate that it is possible to synthesize ACs with their good adsorption capacity of CO_2 [15,31,32,46]. Previous studies showed that the AC adsorbents and modified AC with amine groups showed different CO_2 adsorption capacity based on the textural properties of the AC (i.e. BET surface area, pore volume and the pore size distribution) [32,46]. Table 5 shows the comparison of the CO_2 adsorption capacity of different ACs. As can be seen from this table, it is obvious that HK sample shows highest CO_2 adsorption capacity of up to 4.10 mmol/g at 1 bar and 303 K, compared with those in previous studies of making AC from the same activating agents. A study showed that the surface modification of AC from commercial palm shell-based granular AC with ammonia gas at 800 °C improved the adsorption capacity of CO_2 onto the OXA-800 of up to 3.86 mmol/g at 1 bar and 303 K [31]. In other study, the adsorption of CO_2 and CH_4 on AC from coconut-shells was investigated in the pressure range of 0–2 bar [15]. This study showed that that the modified AC with alkali solution had the highest CO_2 adsorption value of 2.55 mmol/g at 2 bar and 298 K. In other study, the surface modification of ACs using ammonia impregnation produced high quality AC with large surface area for evaluation of CO_2 adsorption performance [26]. This study reported that the CO_2 capture capacities of up to 2.92 and 3.22 mmol/g for origin and modified ACs, respectively, could be obtained at 1 bar and 298 K. In the present study, we prepared a series of ACs from Eucalyptus wood using H_3PO_4, $ZnCl_2$ and KOH. The CO_2 adsorption capacity of prepared AC sample ($H_{1.5}$ and H_2) in this study was highest when compared to other types of AC reported previously in the literature (Table 5). For example, AC from biomass residues and sewage sludge was studied for the treatment of biomass chars by means of physical activation with CO_2 and amination and its adsorption capacity for CO_2 [53]. It was reported that a maximum CO_2 adsorption capacity of about 2.24 mmol/g obtained at 1 bar and 298 K, while carbons developed from sewage sludge showed a lower CO_2 adsorption of about 0.31 mmol/g. A study investigated on the modification of AC by using monoethanolamine (MEA) impregnation in order to improve their adsorption properties toward CO_2 [54]. Their results demonstrated that the modification of AC decreased CO_2 adsorption capacity from 188 to 1.02 mmol/g at 1 bar and 2998 K, which

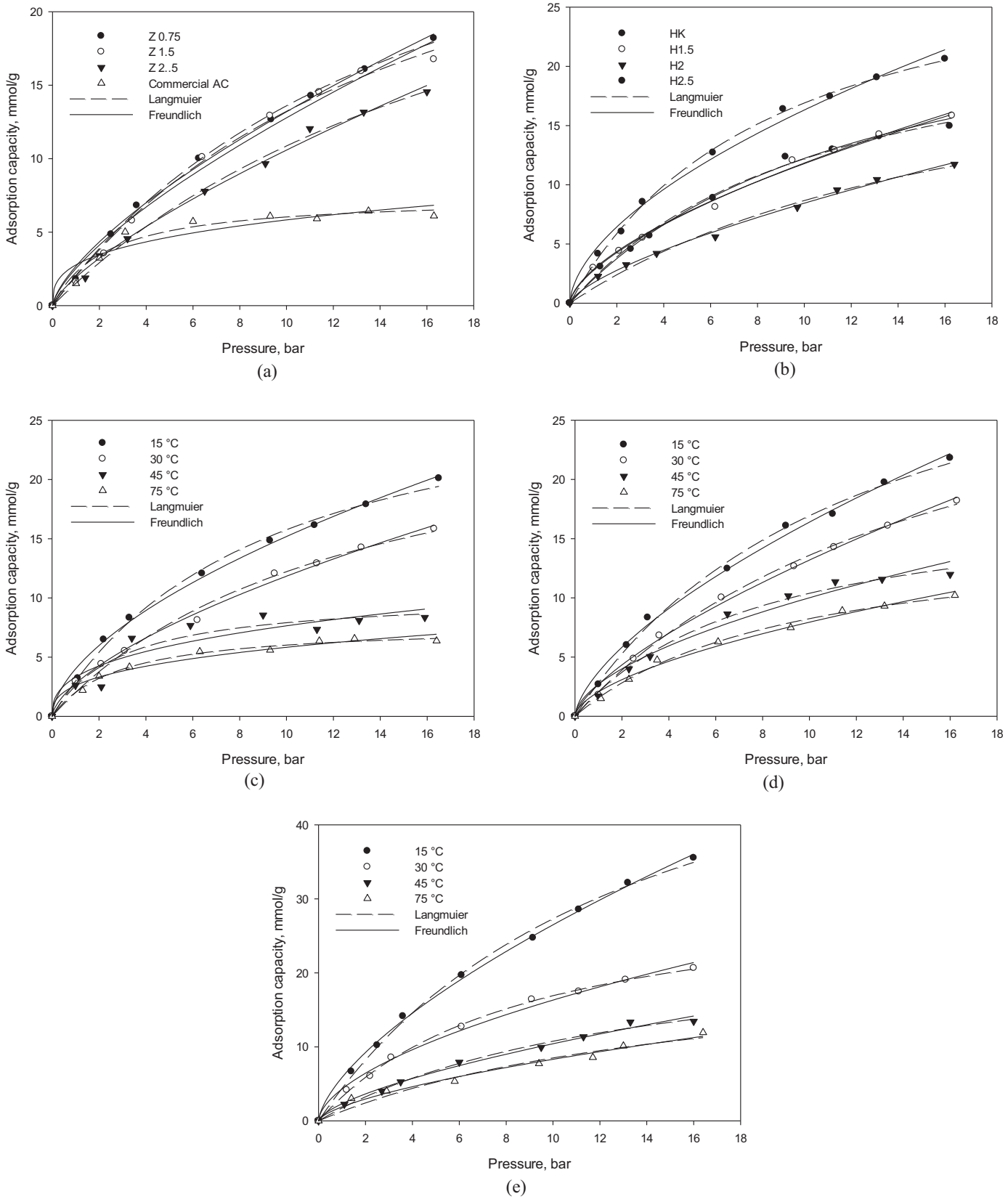

Fig. 5. Curve fitting with Langmuir and Freundlich models of CO_2 adsorption isotherms onto activated carbon from eucalyptus wood at different impregnation ratios of (a) $ZnCl_2$, (b) H_3PO_4 and KOH at 303 K and at different temperatures of (c) H_3PO_4, (d) $ZnCl_2$, and (e) KOH.

Table 4
Parameters of Langmuir and Freundlich models for CO_2 adsorption onto the AC.

Activating agent	Impregnation ratio	Temperature (°C)	Langmuir			Freundlich		
			K_a (l/mol)	q_m (mmol/g)	R^2	K_f	n	R^2
H_3PO_4	1.5	30	0.08	26.04	0.99	2.84	1.61	0.98
	2	15	0.01	30.26	0.99	3.99	1.72	0.99
		30	0.08	28.01	0.99	2.75	1.57	0.99
		45	0.33	10.26	0.91	3.3	2.74	0.87
		75	0.35	7.70	0.99	2.6	2.85	0.97
	2.5	30	0.05	25.02	0.98	1.71	1.44	0.99
$ZnCl_2$	0.75	15	0.08	37.97	0.99	3.72	1.55	0.99
		30	0.06	36.16	0.99	2.68	1.44	0.99
		45	0.12	18.87	0.99	2.69	1.75	0.97
		75	0.1	15.86	0.99	2.05	1.7	0.98
	1.5	30	0.06	34.80	0.99	2.52	1.42	0.98
	2.5	30	0.04	34.19	0.99	1.93	1.35	0.99
KOH	3.5	15	0.07	65.37	0.99	5.86	1.52	0.99
		30	0.11	31.89	0.99	4.31	1.73	0.99
		45	0.07	25.49	0.99	2.31	1.52	0.99
		75	0.05	22.73	0.96	1.88	1.55	0.98
Commercial AC	–	30	0.43	7.42	0.96	2.77	3.09	0.90

Table 5
Comparison of adsorption capacity of CO_2 on different AC.

Adsorbent	Adsorption capacity (mmol/g)	Pressure (bar)	Temperature (°C)	Ref.
[a]L-A850 (40%)	0.31	1	25	[53]
L-A850 (40%)-PEI	0.31			
[b]AOS char	2.06			
AOS-NH_2	2.24			
AC	2.92	1	25	[25]
AAC	3.22			
[c]P-AC	2.55	2	25	[15]
OXA-800	3.86	1	30	[30]
MSC-30	2.27	1	28	[54]
G08H	1.54			
AC	1.88	1	25	[55]
AC/MEA	1.02	1		
AC–MEA	1.54	1	30	[56]
Commercial AC	1.50	1	30	This study
HK	4.10			
$H_{1.5}$	2.36			
H_2	2.98			
$H_{2.5}$	1.88			
$Z_{0.75}$	1.90			
$Z_{1.5}$	1.61			
$Z_{2.5}$	1.34			

[a] AC from sewage sludge (L).
[b] AC from biomass residues (AOS).
[c] AC from coconut-shells.

have comparable agreement with the CO_2 adsorption capacity of $Z_{0.75}$, $Z_{1.5}$ and $Z_{2.5}$ samples.

4. Conclusions

Activated carbons (ACs) were prepared by impregnation of *E. camaldulensis* wood with H_3PO_4, $ZnCl_2$ and KOH. It was found that the activating agent and its concentration strongly influence the textural characteristics of the eucalyptus wood based AC. The BET surface area and porosity increased in this order: KOH > H_3PO_4 > $ZnCl_2$. The best activating agent for preparing AC as CO_2 adsorbent in terms of producing the biggest BET surface area and a high percentage of micropore volume was KOH. The lowest value of micropore content was attained with the high impregnation H_3PO_4 ratio activated samples. AC is identified as being an appropriate adsorbent for CO_2 adsorption due to its big surface area and highly microporous structure. The adsorption capacity of CO_2 at the different pressures and temperatures onto prepared AC samples was studied. The Freundlich and Langmuir models were used to describe the behavior of CO_2 adsorption onto AC. The results show that the lowest temperature and a high micropore content enhanced the amount of CO_2 adsorbed by AC adsorbents. The CO_2 adsorption capacity of 4.1 mmol/g obtained for the prepared AC (HK sample) was much higher than that for commercial AC (1.5 mmol/g) at 1 bar and 303 K.

Acknowledgments

This work was supported by Tarbiat Modares University (TMU) of Iran. The authors gratefully acknowledge the contributions of Dr. Mohammad Ali Ebrahimi Nik, Soodabeh Khalili, Sarah Heidari and all the staff members in the Central Laboratory of the Faculty of Natural Resources Faculty in TMU, and Ellen Vuosalo Tavakoli for the final editing of the English text.

References

[1] Diao Y, Walawender WP, Fan LT. Activated carbons prepared from phosphoric acid activation of grain sorghum. Bioresour Technol 2002;81:45–52.
[2] Liou T-H. Development of mesoporous structure and high adsorption capacity of biomass-based activated carbon by phosphoric acid and zinc chloride activation. Chem Eng J 2010;158:129–42.
[3] Arami-Niya A, Daud WMAW, Mjalli FS. Using granular activated carbon prepared from oil palm shell by $ZnCl_2$ and physical activation for methane adsorption. J Anal Appl Pyrolysis 2010;89:197–203.
[4] Nahil MA, Williams PT. Pore characteristics of activated carbons from the phosphoric acid chemical activation of cotton stalks. Biomass Bioenergy 2012;37:142–9.
[5] Wang K, Li C, San H, Do DD. The importance of finite adsorption kinetics in the sorption of hydrocarbon gases onto a nutshell-derived activated carbon. Chem Eng Sci 2007;62:6836–42.
[6] Khalili NR, Campbell M, Sandi G, Golaś J. Production of micro- and mesoporous activated carbon from paper mill sludge: I. Effect of zinc chloride activation. Carbon 2000;38:1905–15.
[7] El-Hendawy A-NA, Alexander AJ, Andrews RJ, Forrest G. Effects of activation schemes on porous, surface and thermal properties of activated carbons prepared from cotton stalks. J Anal Appl Pyrolysis 2008;82:272–8.
[8] Girgis BS, El-Hendawy A-NA. Porosity development in activated carbons obtained from date pits under chemical activation with phosphoric acid. Microporous Mesoporous Mater 2002;52:105–17.
[9] Liu W-J, Zeng F-X, Jiang H, Zhang X-S. Preparation of high adsorption capacity bio-chars from waste biomass. Bioresour Technol 2011;102:8247–52.
[10] Bagheri N, Abedi J. Preparation of high surface area activated carbon from corn by chemical activation using potassium hydroxide. Chem Eng Res Des 2009;87:1059–64.

[11] Nakagawa Y, Molina-Sabio M, Rodríguez-Reinoso F. Modification of the porous structure along the preparation of activated carbon monoliths with H_3PO_4 and $ZnCl_2$. Microporous Mesoporous Mater 2007;103:29–34.
[12] Martins AF, Cardoso AdL, Stahl JA, Diniz J. Low temperature conversion of rice husks, eucalyptus sawdust and peach stones for the production of carbon-like adsorbent. Bioresour Technol 2007;98:1095–100.
[13] Bouhamed F, Elouear Z, Bouzid J. Adsorptive removal of copper(II) from aqueous solutions on activated carbon prepared from Tunisian date stones: Equilibrium, kinetics and thermodynamics. J Taiwan Inst Chem Eng 2012;43:741–9.
[14] Plaza MG, Pevida C, Martín CF, Fermoso J, Pis JJ, Rubiera F. Developing almond shell-derived activated carbons as CO_2 adsorbents. Sep Purif Technol 2010;71:102–6.
[15] Yang H, Gong M, Chen Y. Preparation of activated carbons and their adsorption properties for greenhouse gases: CH_4 and CO_2. J Nat Gas Chem 2011;20:460–4.
[16] Girgis BS, Khalil LB, Tawfik TAM. Activated carbon from sugar cane bagasse by carbonization in the presence of inorganic acids. J Chem Technol Biotechnol 1994;61:87–92.
[17] Foo KY, Hameed BH. Preparation and characterization of activated carbon from pistachio nut shells via microwave-induced chemical activation. Biomass Bioenergy 2011;35:3257–61.
[18] Wu F-C, Tseng R-L, Hu C-C. Comparisons of pore properties and adsorption performance of KOH-activated and steam-activated carbons. Microporous Mesoporous Mater 2005;80:95–106.
[19] Patnukao P, Pavasant P. Activated carbon from *Eucalyptus camaldulensis* Dehn bark using phosphoric acid activation. Bioresour Technol 2008;99:8540–3.
[20] Ngernyen Y, Tangsathitkulchai C, Tangsathitkulchai M. Porous properties of activated carbon produced from Eucalyptus and Wattle wood by carbon dioxide activation. Korean J Chem Eng 2006;23:1046–54.
[21] Tancredi N, Cordero T, Rodríguez-Mirasol J, Rodríguez JJ. Activated carbons from Uruguayan eucalyptus wood. Fuel 1996;75:1701–6.
[22] Elyounssi K, Collard F-X, Mateke J-aN, Blin J. Improvement of charcoal yield by two-step pyrolysis on eucalyptus wood: a thermogravimetric study. Fuel 2012;96:161–7.
[23] Romanos J, Beckner M, Rash T, Firlej L, Kuchta B, Yu P, et al. Nanospace engineering of KOH activated carbon. Nanotechnology 2012;23:015401.
[24] Shafeeyan MS, Wan Daud WMA, Houshmand A, Arami-Niya A. The application of response surface methodology to optimize the amination of activated carbon for the preparation of carbon dioxide adsorbents. Fuel 2012;94: 465–72.
[25] Jang D-I, Park S-J. Influence of nickel oxide on carbon dioxide adsorption behaviors of activated carbons. Fuel 2012;102:439–44.
[26] Zhang Z, Xu M, Wang H, Li Z. Enhancement of CO_2 adsorption on high surface area activated carbon modified by N_2, H_2 and ammonia. Chem Eng J 2010;160:571–7.
[27] Plaza MG, García S, Rubiera F, Pis JJ, Pevida C. Evaluation of ammonia modified and conventionally activated biomass based carbons as CO_2 adsorbents in postcombustion conditions. Sep Purif Technol 2011;80:96–104.
[28] Hedin N, Chen L, Laaksonen A. Sorbents for CO_2 capture from flue gas-aspects from materials and theoretical chemistry. Nanoscale 2010;2:1819–41.
[29] Li J-R, Ma Y, McCarthy MC, Sculley J, Yu J, Jeong H-K, et al. Carbon dioxide capture-related gas adsorption and separation in metal-organic frameworks. Coord Chem Rev 2011;255:1791–823.
[30] D'Alessandro DM, Smit B, Long JR. Carbon dioxide capture: prospects for new materials. Angew Chem Int Ed 2010;49:6058–82.
[31] Shafeeyan MS, Daud WMAW, Houshmand A, Arami-Niya A. Ammonia modification of activated carbon to enhance carbon dioxide adsorption: effect of pre-oxidation. Appl Surf Sci 2011;257:3936–42.
[32] Sevilla M, Fuertes AB. CO_2 adsorption by activated templated carbons. J Colloid Interface Sci 2012;366:147–54.
[33] Shen C, Grande CA, Li P, Yu J, Rodrigues AE. Adsorption equilibria and kinetics of CO_2 and N_2 on activated carbon beads. Chem Eng J 2010;160:398–407.
[34] Dobele G, Dizhbite T, Gil MV, Volperts A, Centeno TA. Production of nanoporous carbons from wood processing wastes and their use in supercapacitors and CO_2 capture. Biomass Bioenergy 2012;46:145–54.
[35] Pevida C, Plaza MG, Arias B, Fermoso J, Rubiera F, Pis JJ. Surface modification of activated carbons for CO_2 capture. Appl Surf Sci 2008;254:7165–72.
[36] Li F, Yi H, Tang X, Ning P, Yu Q, Kang D. Adsorption of carbon dioxide by coconut activated carbon modified with Cu/Ce. Journal of Rare Earths 2010;28:334–7.
[37] Li W, Peng J, Zhang L, Xia H, Li N, Yang K, et al. Investigations on carbonization processes of plain tobacco stems and H_3PO_4-impregnated tobacco stems used for the preparation of activated carbons with H_3PO_4 activation. Ind Crops Prod 2008;28:73–80.
[38] Nieto-Delgado C, Terrones M, Rangel-Mendez JR. Development of highly microporous activated carbon from the alcoholic beverage industry organic by-products. Biomass Bioenergy 2011;35:103–12.
[39] Guo J, Lua A. Textural characterization of activated carbons prepared from oil-palm stones pre-treated with various impregnating agents. J Porous Mater 2000;7:491–7.
[40] Timur S, Kantarli IC, Onenc S, Yanik J. Characterization and application of activated carbon produced from oak cups pulp. J Anal Appl Pyrolysis 2010;89:129–36.
[41] Demirbas E, Kobya M, Sulak MT. Adsorption kinetics of a basic dye from aqueous solutions onto apricot stone activated carbon. Bioresour Technol 2008;99:5368–73.
[42] Lillo-Ródenas MA, Cazorla-Amorós D, Linares-Solano A. Understanding chemical reactions between carbons and NaOH and KOH: an insight into the chemical activation mechanism. Carbon 2003;41:267–75.
[43] Molina-Sabio M, Rodríguez-Reinoso F. Role of chemical activation in the development of carbon porosity. Colloid Surf Physicochem Eng Aspects 2004;241:15–25.
[44] Guo J, Lua AC. Surface functional groups on oil-palm-shell adsorbents prepared by H_3PO4 and KOH activation and their effects on adsorptive capacity. Chem Eng Res Des 2003;81:585–90.
[45] Shaarani FW, Hameed BH. Ammonia-modified activated carbon for the adsorption of 2,4-dichlorophenol. Chem Eng J 2011;169:180–5.
[46] Shafeeyan MS, Daud WMAW, Houshmand A, Shamiri A. A review on surface modification of activated carbon for carbon dioxide adsorption. J Anal Appl Pyrolysis 2010;89:143–51.
[47] Yong Z, Mata V, Rodrigues ArE. Adsorption of carbon dioxide at high temperature—a review. Sep Purif Technol 2002;26:195–205.
[48] Houshmand A, Daud W, Lee M-G, Shafeeyan M. Carbon dioxide capture with amine-grafted activated carbon. Water Air Soil Pollut 2012;223:827–35.
[49] Grondein A, Bélanger D. Chemical modification of carbon powders with aminophenyl and aryl-aliphatic amine groups by reduction of in situ generated diazonium cations: applicability of the grafted powder towards CO_2 capture. Fuel 2011;90:2684–93.
[50] Lee S-Y, Park S-J. Effect of temperature on activated carbon nanotubes for hydrogen storage behaviors. Int J Hydrogen Energy 2010;35:6757–62.
[51] Lee S-Y, Park S-J. Preparation and characterization of ordered porous carbons for increasing hydrogen storage behaviors. J Solid State Chem 2011;184:2655–60.
[52] Lee S-Y, Park S-J. Determination of the optimal pore size for improved CO_2 adsorption in activated carbon fibers. J Colloid Interface Sci 2013;389:230–5.
[53] Plaza MGP C, Arias B, Casal MD, Martín CF, Fermoso J, Rubiera F, et al. Different approaches for the development of low-cost CO_2 adsorbents. J Environ Eng 2009;135:426–32.
[54] Bezerra D, Oliveira R, Vieira R, Cavalcante Jr C, Azevedo DS. Adsorption of CO_2 on nitrogen-enriched activated carbon and zeolite 13X. Adsorption 2011;17:235–46.
[55] Yong Z, Mata V, Rodrigues A. Adsorption of Carbon Dioxide on Chemically Modified High Surface Area Carbon-Based Adsorbents at High Temperature. Adsorption 2001;7:41–50.
[56] Mercedes Maroto-Valer M, Lu Z, Zhang Y, Tang Z. Sorbents for CO_2 capture from high carbon fly ashes. Waste Management 2008;28:2320–8.